# Requirement of open headpiece conformation for activation of leukocyte integrin $\alpha_X\beta_2$

Xing Chen[a], Can Xie[a], Noritaka Nishida[a,1], Zongli Li[b], Thomas Walz[b], and Timothy A. Springer[a,2]

[a]Immune Disease Institute, Children's Hospital Boston and Department of Pathology and [b]Howard Hughes Medical Institute and Department of Cell Biology, Harvard Medical School, Boston, MA 02115

Contributed by Timothy A. Springer, June 18, 2010 (sent for review April 24, 2010)

**Negative stain electron microscopy (EM) and adhesion assays show that $\alpha_X\beta_2$ integrin activation requires headpiece opening as well as extension. An extension-inducing Fab to the $\beta_2$ leg, in combination with representative activating and inhibitory Fabs, were examined for effect on the equilibrium between the open and closed headpiece conformations. The two activating Fabs stabilized the open headpiece conformation. Conversely, two different inhibitory Fabs stabilized the closed headpiece conformation. Adhesion assays revealed that $\alpha_x\beta_2$ in the extended-open headpiece conformation had high affinity for ligand, whereas both the bent conformation and the extended-closed headpiece conformation represented the low affinity state. Intermediate integrin affinity appears to result not from a single conformational state, but from a mixture of equilibrating conformational states.**

Integrins are a major family of αβ heterodimeric, cell surface adhesion receptors that transmit both chemical signals and mechanical forces bidirectionally across the plasma membrane (1). The integrin α and β subunits are each type I transmembrane proteins with large N-terminal extracellular domains, single-spanning transmembrane domains, and usually short C-terminal cytoplasmic domains (Fig. 1 *A–C*). The $\beta_2$ integrin subfamily, $\alpha_D\beta_2$, $\alpha_M\beta_2$ (CR3, Mac-1), $\alpha_L\beta_2$ (LFA-1), and $\alpha_X\beta_2$ (CR4, p150,95), is exclusively expressed on leukocytes. All $\beta_2$ integrins contain an inserted I domain in the α subunit, which is the ligand-binding domain. The head comprises the α-subunit β-propeller and αI domains, and the β-subunit βI domain (Fig. 1*D*). The upper legs comprise the α-subunit thigh domain, and the β-subunit PSI, hybrid, and I-EGF1 domains. The head and upper legs together are called the headpiece. The lower legs comprise the α-subunit calf-1 and calf-2 domains, and the β-subunit I-EGF domains 2–4 and β-tail domain (Fig. 1*D*).

Crystal structures of the ectodomain of both αI-less (2, 3) and αI-containing integrins (4) revealed a bent conformation, in which the lower α and β legs fold back against the head and upper legs (Fig. 1*A*). It is believed that the bent conformation represents the physiological low affinity state, whereas during activation, integrins extend with a switchblade-like motion (5–9). EM images of the αI-less integrin, $\alpha_V\beta_3$, showed the extended conformation upon activation by $Mn^{2+}$ or ligand binding (6).

Over the years, an array of mAbs has been developed that can inhibit, induce, or report $\beta_2$ integrin activation on cell surfaces. Therefore, correlating the functional effects of mAbs on intact cells with their effects on integrin conformational changes revealed by EM provides a powerful method for studying the mechanism of integrin activation. mAbs that bind to epitopes that are buried in the bent conformation can induce extension, as found with CBR LFA-1/2 Fab to I-EGF3; or report extension, as found with KIM127 Fab to I-EGF2 (5, 8, 10). Upon extension, two headpiece conformations were observed: closed, as when bent (Fig. 1 *B* and *E*), and open, with the hybrid domain swung out (Fig. 1 *C* and *F*) (6, 8).

The open headpiece conformation has been widely speculated to be the activated state with high affinity for ligand, because ligand binding induces and stabilizes the open headpiece conformation (6, 11–13). Moreover, mutations that stabilize the open headpiece conformation activate ligand binding (14, 15). However, direct evidence for distinct functional roles for the extended conformation with the closed headpiece (Fig. 1*B*) and the extended conformation with the open headpiece (Fig. 1*C*) is yet to be acquired for any integrin. Furthermore, there has been much speculation about an intermediate affinity state between the bent, low affinity and the activated, high affinity states. At the leading edge of migrating T lymphocytes, a distinct population of LFA-1 was defined as in an intermediate affinity state by the exposure of different monoclonal antibody epitopes (16). Lateral mobility measurements of LFA-1 on T cell surfaces suggested an intermediate conformational state with distinct diffusion profile (17). In vitro flow chamber experiments showed that an intermediate affinity of LFA-1 on lymphocytes could be induced by immobilized chemokine (18). Moreover, different affinity and conformational states of LFA-1 have been suggested on the basis of differential effects of antibodies and metal ions on binding to the higher affinity ligand ICAM-1 and the lower affinity ligand ICAM-3 (19–22). Nevertheless, it remains unclear which conformational state corresponds to the observed intermediate affinity and what affinity state the extended-closed headpiece conformation represents. Finally, the adhesiveness of the bent conformation, the extended-closed headpiece conformation, and the extended-open headpiece conformation has never been compared for any integrin.

We herein examine the effects of representative activating and inhibitory Fabs on the headpiece conformation and function of $\alpha_X\beta_2$ integrin. The results show that extension in the absence of headpiece opening is not sufficient for integrin activation and that the open headpiece conformation is required for $\alpha_X\beta_2$ integrin activation.

## Results

We used a previously described, secreted, physiologically relevant $\alpha_x\beta_2$ ectodomain construct (4, 8). The construct contains ACID/BASE coiled coils appended to the C termini of the α and β subunits (Fig. 1*D*). The coiled-coil clasp mimics the association between the α- and β-subunit transmembrane and cytoplasmic domains in intact integrins (Fig. 1 *A–C*). Below, we describe the conformation of this $\alpha_X\beta_2$ construct, alone or complexed with CBR LFA-1/2 Fab to induce extension and with a second Fab to test the effect on headpiece conformation. Purified $\alpha_X\beta_2$ protein was incubated with excess Fabs, and complexes were isolated by Superdex 200 chromatography (Fig. 1*G*) and immediately subjected to negative staining with uranyl formate (Fig. S1 *A–D*) (23). Two to six thousand particles were picked interactively and subjected to multireference alignment and *K*-means classification specifying 50 classes (Fig. S2 *A–F*). The percentages of particles in each conformation represented below were estimated by summing particles in each class for a given conformation and dividing

Author contributions: X.C. and T.A.S. designed research; X.C., C.X., N.N., and Z.L. performed research and analyzed data; and X.C., T.W., and T.A.S. wrote the paper.

The authors declare no conflict of interest.

[1]Present address: University of Tokyo, Hongo, Bunkyo-ku, Tokyo 113-0033, Japan.

[2]To whom correspondence should be addressed. E-mail: springer@idi.harvard.edu.

This article contains supporting information online at www.pnas.org/lookup/suppl/doi:10.1073/pnas.1008663107/-/DCSupplemental.

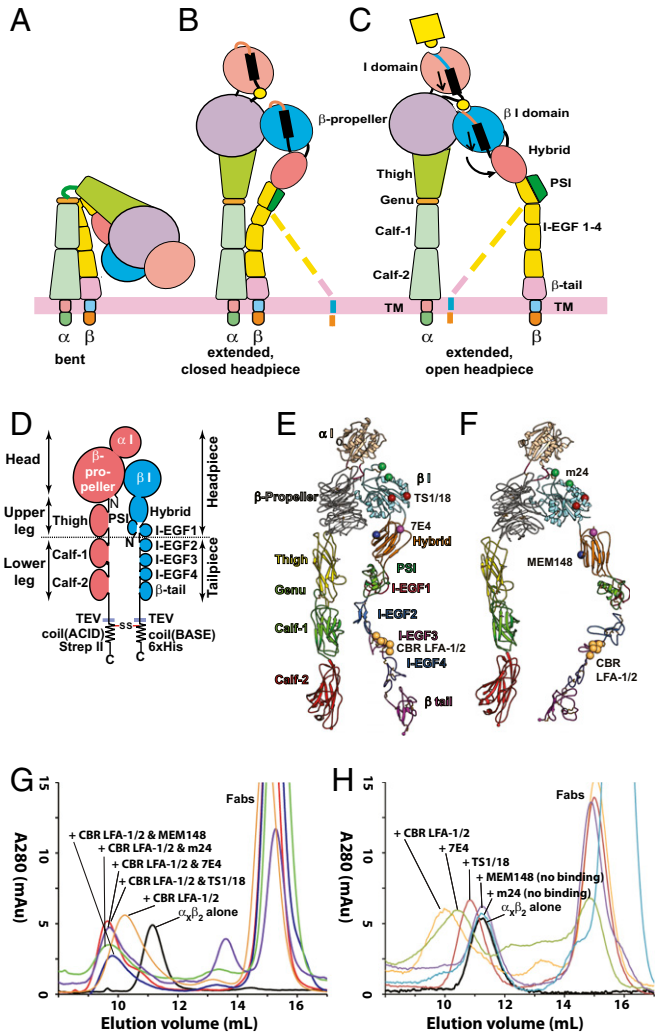


**Fig. 1.** Integrin conformational states and preparation of $\alpha_x\beta_2$–Fab complexes. (*A–C*) Schematic of three conformational states of integrin. (*D*) Schematic of the $\alpha_x\beta_2$ ectodomain construct used in this study. (*E* and *F*) Ribbon diagrams of the $\alpha_x\beta_2$ ectodomain in extended-closed headpiece (*E*) and extended-open headpiece (*F*) conformations. Spheres show Cα atoms of residues to which epitopes are mapped. Epitopes are labeled in the headpiece conformation for which mAb are found to be specific in this study. Models are based on the bent $\alpha_x\beta_2$ crystal structure (4) and open $\alpha_{IIb}\beta_3$ headpiece (13). (*G* and *H*) Superdex 200 size exclusion chromatography profiles of $\alpha_x\beta_2$ in the absence and presence of the indicated Fabs.

by the total numbers of particles. The most populous classes with most structural details are shown in the main text. In the absence of Fab, more than 95% of particles adopted the same bent conformation (Fig. 2*A* and Fig. S2*A*) as seen in previous $\alpha_X\beta_2$ EM (8) and crystal structures (4). Integrin $\alpha_X\beta_2$ in complex with CBR LFA-1/2 Fab adopted extended conformations (Fig. 2*B* and Fig. S2*B*), as previously reported (8). Two different headpiece conformations, closed and open, were observed in equal proportions (Fig. 2*B*). Particles with the closed headpiece conformation could have their legs either parallel (Fig. 2*B* row 1) or crossed (Fig. 2*B* row 2). Particles with the open headpiece conformation had their legs apart (Fig. 2*B* row 3).

MEM148 is an activation-dependent mAb whose epitope maps to residue Pro-374, on the face of the $\beta_2$ hybrid domain facing the α subunit, i.e., the inner face of the hybrid domain (Fig. 1*F*). MEM148 has been used to activate $\beta_2$ integrins and/or report the activated conformation (21, 24). $\alpha_X\beta_2$ with both CBR LFA-1/2 and MEM148 Fabs eluted earlier in gel filtration than the complex containing only CBR LFA-1/2 Fab (Fig. 1*G*). About 70% of the particles were integrins complexed with both Fabs (Fig. 2*C* row 1). MEM148 bound to the inner side of the hybrid domain, near its junction with the β I domain (Fig. 2*C* row 1), in excellent agreement with mapping of the epitope to Pro-374 (Fig. 1*F*). Importantly, all particles with MEM148 bound adopted the open headpiece conformation (Fig. 2*C* row 1 and Fig. S2*C*).

The remaining 30% of particles produced class averages containing only CBR LFA-1/2 Fab (Fig. 2*C* rows 2–4 and Fig. S2*C*). It is not uncommon for Fab to dissociate from complexes during preparation for EM. This may occur during complex separation from free Fab in gel filtration or before or during EM grid preparation. Similar to the preparation of $\alpha_X\beta_2$–CBR LFA-1/2 complex shown in Fig. 2*B*, approximately equal proportions of particles containing CBR LFA-1/2 Fab and lacking MEM148 Fab adopted closed (14%) and open (16%) headpiece conformations (Fig. 2*C* rows 2–4). For particles with the closed headpiece, the legs were either parallel (Fig. 2*C* row 2) or crossed (Fig. 2*C* row 3), exactly as found in the $\alpha_X\beta_2$–CBR LFA-1/2 Fab preparation (Fig. 2*B* rows 1–2). The particles with the open headpiece conformation lacking MEM148 and containing CBR LFA-1/2 Fab (Fig. 2*C* row 4) also closely resembled those seen in the $\alpha_X\beta_2$–CBR LFA-1/2 Fab preparation (Fig. 2*B* row 3). Thus, the particles without MEM148 serve as an internal control and demonstrate that the presence of only the open headpiece in the particles with MEM148 is a specific consequence of binding MEM148 Fab.

mAb 7E4 also binds to the $\beta_2$ hybrid domain, but in contrast to MEM148 is inhibitory (25, 26). 7E4 binds to residue Val-385, which locates to a loop on the outer face of the hybrid domain, at the interface with the βI domain (Fig. 1*E*). The complex with CBR LFA-1/2 and 7E4 Fabs eluted at a position similar to the complex with CBR LFA-1/2 and MEM148 Fabs (Fig. 1*G*). However, the complex with CBR LFA-1/2 and 7E4 assumed exclusively the extended-closed headpiece conformation (Fig. 3 and Fig. S2*D*). 7E4 Fab bound to the outer face of the hybrid domain located away from the $\alpha_X$ subunit, in agreement with epitope mapping (Fig. 1*E*). The legs in the complex were either parallel (Fig. 3 row 1) or crossed (Fig. 3 row 2). No significant dissociation of 7E4 Fab (less than 5%) was observed (Fig. S2*D*).

m24 is an activation-reporting mAb that binds to the βI domain (27, 28). The epitope of m24 maps to residues in the βI specificity determining loop (Glu-175) and α1-helix (Arg-122) near the β I MIDAS across from the α-subunit interface (Fig. 1*F*). The complex containing both CBR LFA-1/2 and m24 eluted earlier than the complex with CBR LFA-1/2 alone (Fig. 1*G*). Gel filtration of $\alpha_X\beta_2$ plus m24 Fab in the absence of CBR LFA-1/2 showed that the vast majority of $\alpha_X\beta_2$ was unshifted in elution position; however a shoulder may indicate a small amount of complex formation (Fig. 1*H*). Class averages (Fig. S2*E*) containing both m24 and CBR LFA-1/2 Fabs bound to $\alpha_X\beta_2$ exhibited exclusively the extended-open headpiece conformation (Fig. 4 row 1). The m24 Fab bound to the face of the βI domain adjacent to the αI domain, in excellent agreement with epitope localization (Fig. 1*F*). Dissociation of m24 was observed from about 24% of particles. These particles exhibited approximately equal proportions of the closed and open headpiece conformations (Fig. 4 rows 2 and 3), in agreement with the results of the $\alpha_X\beta_2$–CBR LFA-1/2 Fab preparation (Fig. 2*B*).

TS1/18 binds to the βI domain, but in contrast to m24 allosterically inhibits $\beta_2$ integrin activation (27, 29). The epitope maps to residues that are adjacent in the α1 and α7-helices of the βI domain (Arg-133 and Gln-332) (Fig. 1*E*). The formation of the $\alpha_X\beta_2$ complex with CBR LFA-1/2 and TS1/18 was confirmed by gel filtration (Fig. 1*G*). TS1/18 also bound to $\alpha_X\beta_2$ in the absence of CBR LFA-1/2 as shown by earlier elution of the complex than $\alpha_X\beta_2$ alone (Fig. 1*H*). Class averages showed exclusively the extended-closed headpiece conformation (Fig. 5 and Fig. S2*F*). No significant dissociation of CBR LFA-1/2 Fab was observed. The

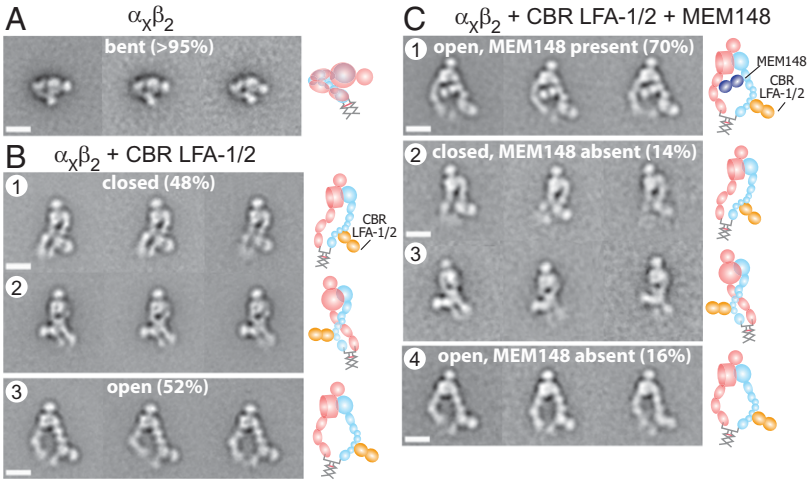


**Fig. 2.** Representative class averages of $\alpha_x\beta_2$ alone, $\alpha_x\beta_2$ with CBR LFA-1/2, and $\alpha_x\beta_2$ with CBR LFA-1/2 and MEM148 Fabs. (*A*) Class averages of $\alpha_x\beta_2$ alone. Most of the particles are in the bent conformation. (*B*) Class averages of the $\alpha_x\beta_2$–CBR LFA-1/2 complex. The particles mostly adopt extended conformations, in which the headpiece is closed with parallel legs (row 1), closed with crossed legs (row 2), or open (row 3). (*C*) Class averages of $\alpha_x\beta_2$ in complex with CBR LFA-1/2 and MEM148 Fabs. Approximately 70% of the particles are complexes with both Fabs, which adopt exclusively the extended-open headpiece conformation (row 1). The remaining 30% of particles are particles with only $\alpha_x\beta_2$–CBR LFA-1/2 Fab, which exhibit exactly the same conformational states (rows 2, 3, and 4), as seen in rows 1, 2, and 3, respectively, in *B*. To the right of each set of class averages, cartoons show the domain arrangement and Fab position. (Scale bar, 10 nm.)

TS1/18 Fab bound to the βI domain near the αI domain. There was slightly more room between the αI domain and the TS1/18 Fab than seen with m24 Fab (compare Fig. 4 row 1 and Fig. 5), consistent with binding of TS1/18 to a residue in the α1-helix (Arg-133) more C-terminal than the residue in the α1-helix (Arg-122) to which m24 binds. Unlike 7E4, only the crossed leg conformation was observed with TS1/18.

Finally, we compared the adhesiveness of $\alpha_X\beta_2$ in different conformations stabilized by Fabs. Purified $\alpha_X\beta_2$ protein was captured on a plastic plate by a rabbit polyclonal anti-velcro antibody against the ACID/BASE coiled coil. The captured $\alpha_X\beta_2$ was then incubated with the same individual Fabs and pairs of Fabs as used in EM. Ligand binding was measured with iC3b-opsonized sheep erythrocytes (Fig. 6). $\alpha_X\beta_2$ with no stimulus showed only background binding to iC3b, confirming the bent conformation had low affinity (Fig. 6*A*). $\alpha_X\beta_2$ activated with 2 mM of $Mn^{2+}$ bound strongly to E-IgM-iC3b (Fig. 6*A*). The $\alpha_X\beta_2$–CBR LFA-1/2 complex showed significant binding to E-IgM-iC3b, although less than $\alpha_X\beta_2$ in $Mn^{2+}$ (Fig. 6*A*). As shown in Fig. 2*B*, the $\alpha_X\beta_2$–CBR LFA-1/2 complex was a mixture of the extended-open headpiece and the extended-closed headpiece conformations. The $\alpha_X\beta_2$ complexes containing CBR LFA-1/2 and MEM148, or CBR LFA-1/2 and m24 showed the highest binding of E-IgM-iC3b (Fig. 6*A*). In these two conditions, $\alpha_X\beta_2$ was seen by EM to be in the extended-open headpiece conformation (Figs. 2*C* and 4). By contrast, the $\alpha_X\beta_2$ complexes containing CBR LFA-1/2 and 7E4 Fabs, or CBR LFA-1/2 and TS1/18 Fabs exhibited adhesiveness significantly lower than that of the $\alpha_X\beta_2$–CBR LFA-1/2 complex (Fig. 6*A*). These results demonstrated that extension itself is not sufficient for high affinity and that the extended-open headpiece conformation is the activated, high affinity state. Thus the level of adhesiveness correlated with the proportion of extended integrin with the open headpiece conformation.

We were curious about the observation that binding of E-IgM-iC3b was higher to $\alpha_X\beta_2$ incubated with CBR LFA-1/2 and TS1/18 or 7E4 Fabs than to $\alpha_X\beta_2$ with no stimulus. This might be explained by E-IgM-iC3b binding to extended-closed $\alpha_X\beta_2$ bound to TS1/18 Fab, suggesting that the extended-closed headpiece conformation could have intermediate affinity. Alternatively, E-IgM-iC3b might be competing with TS1/18 Fab and stabilizing the binding to the extended-open headpiece conformation. If this were true, then the extended-closed headpiece conformation would represent the low affinity state. To distinguish between these alternatives, we varied the concentration of TS1/18 Fab while maintaining the concentration of CBR LFA-1/2 at 10 μg/mL. With increasing TS1/18 Fab concentrations, the binding of E-IgM-iC3b decreased in a dose-dependent manner, until reaching a level similar to that of the unstimulated control in the bent conformation (Fig. 6*B*). These results suggest that the extended-closed headpiece conformation has low affinity for ligand, similar to the bent conformation.

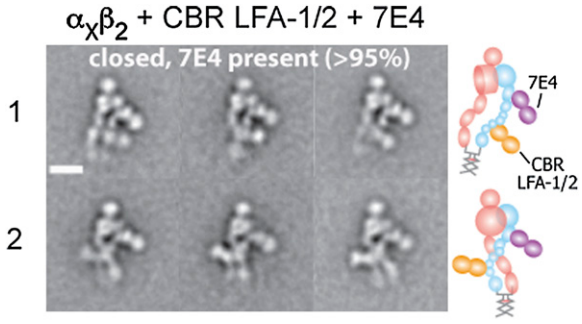


**Fig. 3.** Representative class averages of $\alpha_x\beta_2$ in complex with CBR LFA-1/2 and 7E4 Fabs. The particles mostly adopt the extended-closed headpiece conformation. The leg conformations are either parallel (row 1) or crossed (row 2). To the right of each set of class averages, cartoons show the domain arrangement and Fab position. (Scale bar, 10 nm.)

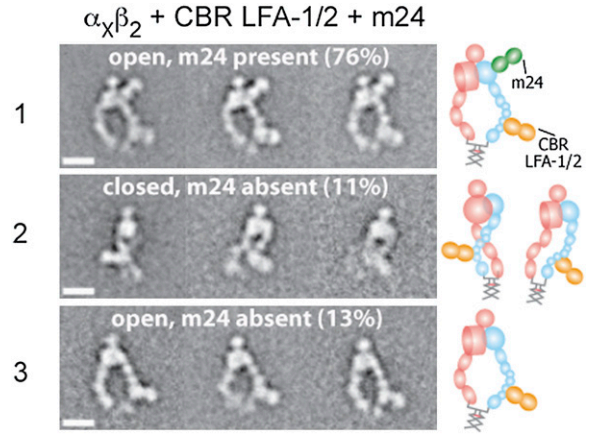


**Fig. 4.** Representative class averages of $\alpha_x\beta_2$ in complex with CBR LFA-1/2 and m24 Fabs. About 76% of the particles contain both Fabs, which assume the extended-open headpiece conformation (row 1). The remaining 24% of the particles contain only CBR LFA-1/2 Fab (rows 2 and 3). To the right of each set of class averages, cartoons show the domain arrangement and Fab position. (Scale bar, 10 nm.)

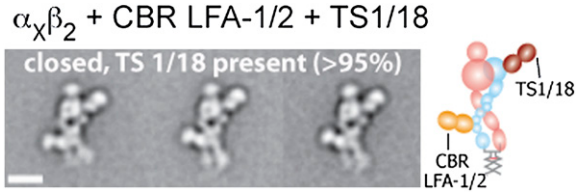


**Fig. 5.** Representative class averages of $\alpha_x\beta_2$ in complex with CBR LFA-1/2 and TS1/18 Fabs. The particles mostly adopt the extended-closed headpiece conformation. The particles only exhibit the crossed leg conformation. To the right of the class average, the cartoon shows the domain arrangement and Fab position. (Scale bar, 10 nm.)

We also examined how the Fabs individually affected the adhesiveness of $\alpha_X\beta_2$ (Fig. 6*C*). Incubation of $\alpha_X\beta_2$ with MEM148 did not increase binding of E-IgM-iC3b, which is in excellent agreement with the gel filtration results showing that MEM148 did not bind to $\alpha_X\beta_2$ without CBR LFA-1/2 present (Fig. 1*H*). Although the vast majority of $\alpha_X\beta_2$ did not bind to m24, a shoulder eluting earlier than $\alpha_X\beta_2$ (Fig. 1*H*) may correspond to a small amount of complex formation and correlate with slight enhancement of ligand binding by m24 alone (Fig. 6*C*). KIM127, a known extension reporting mAb that can only bind to extended $\alpha_X\beta_2$ (5, 8), showed no significant increase in E-IgM-iC3b binding. Gel filtration demonstrated that 7E4 and TS1/18 were able to bind to $\alpha_X\beta_2$ in the absence of CBR LFA-1/2; the $\alpha_X\beta_2$–7E4 complex and $\alpha_X\beta_2$–TS1/18 eluted earlier than $\alpha_X\beta_2$ alone (Fig. 1*H*). $\alpha_X\beta_2$ incubated with the inhibitory 7E4 and TS1/18 Fab showed only background binding of E-IgM-iC3b (Fig. 6*C*).

## Discussion

The α I-less integrin $\alpha_V\beta_3$ and the αI integrin $\alpha_X\beta_2$ show three overall conformational states: a bent conformation with a closed headpiece (bent), an extended conformation with a closed headpiece (extended, closed), and an extended conformation with an open headpiece (extended, open) (2, 6, 8). The extended-open conformation was inferred to be high affinity, because ligand binding induces headpiece opening (6, 11–13), and mutations that stabilize the open headpiece relative to the closed headpiece are activating (14, 15, 30). However, the affinity state of the extended-closed conformation was unclear.

mAbs to integrins produced over the last 30 yr are a valuable resource, because their effects on integrin function on intact cells are well characterized (31). Previously, we have used the antibodies CBR LFA-1/2 and KIM127, which bind to the lower $\beta_2$ leg to show that extension is closely associated with $\beta_2$ integrin activation (8). Here, we have probed the relative importance of the extended-closed and extended-open conformations, using activating and inhibitory mAbs to the integrin headpiece. These antibodies recognize epitopes in the two domains in the integrin headpiece that undergo shape shifting between the open and closed conformations, the βI and hybrid domains.

We used CBR LFA-1/2 in this study to induce integrin extension. The epitope of CBR LFA-1/2 is located on the I-EGF3 domain, and is buried in an interface with the hybrid domain in the bent conformation, but exposed upon integrin extension (Fig. 1 *E* and *F*) (4, 5). CBR LFA-1/2 binds both the extended-open and the extended-closed conformations and is compatible with the binding of both the activation-associated and the inhibitory antibodies that are directed to the hybrid and βI domains.

The C-terminal coiled-coil clasp used here was chosen to mimic constraints imposed in native $\alpha_X\beta_2$ by the associating α- and β-subunit transmembrane domains. Four $\alpha_X\beta_2$ ectodomain constructs with different C-terminal clasps have been previously compared in negative stain EM (4). When a C-terminal coiled coil is present, as in the construct studied here, all particles are in the bent conformation; however, extension can be readily induced with Fabs or other agents (4, 8).

Two activation-associated antibodies bind to the open headpiece and not the closed headpiece conformation. MEM148 is a reporter of LFA-1 activation on intact cells, and can enhance LFA-1 adhesiveness in combination with $Mg^{2+}$/EDTA (21, 24). This antibody binds to Pro-374 on the inner face of the hybrid domain, i.e., the face closest to the α-subunit β-propeller domain (21) (Fig. 1*F*). This residue is in a loop between two β-strands in the hybrid domain that do not undergo conformational change upon headpiece opening (3, 13). The EM class averages show that the MEM148 Fab occupies much of the space between the $\beta_2$ hybrid domain and the $\alpha_X$ β-propeller and thigh domains in the open headpiece conformation. It appears that in the closed headpiece (Fig. 1*E*), there is insufficient room between these domains for the MEM148 Fab to bind. MEM148 did not bind to bent $\alpha_X\beta_2$, in agreement with studies that show the presence of the closed headpiece in the bent conformation of $\alpha_X\beta_2$ (4). m24 also is a reporter of $\beta_2$ integrin activation and is widely used to detect high affinity LFA-1 on intact cells (16, 32, 33). m24 binds to residues near the MIDAS and in the βI domain, including Arg-122 and Glu-175 (Fig. 1*F*) (27). Arg-122 is in the α1-helix, which includes residues that bind the MIDAS and ADMIDAS metal ions, and which move in shape shifting to the open conformation. These residues are well exposed to solvent in both the open and closed headpiece and in the bent integrin conformation (4). The absolute selectivity of m24 for the open headpiece conformation must therefore reflect specificity for a conformation of its epitope, i.e., the exact shape of these residues and the surrounding region that is bound by the Fab, that is unique to the open headpiece. The lack or very small amount of m24 binding to bent $\alpha_X\beta_2$ is again consistent with evidence that bent $\alpha_X\beta_2$ has a closed headpiece (4).

Two inhibitory antibodies were completely specific for the closed headpiece conformation. 7E4 inhibits LFA-1 activation on intact cells and can abrogate phorbol ester- or mAb KIM185-activated, $\beta_2$ integrin-mediated cell adhesion (26, 34). 7E4 recognizes Val-385 in a hybrid domain loop adjacent to its interface with the βI domain (Fig. 1 *E* and *F*) (26). Val-385 and the surrounding region are well exposed to solvent in the bent, extended-closed and extended-open integrin conformations (4). However, Val-385 is in a loop of the hybrid domain that is in the interface with βI domain,

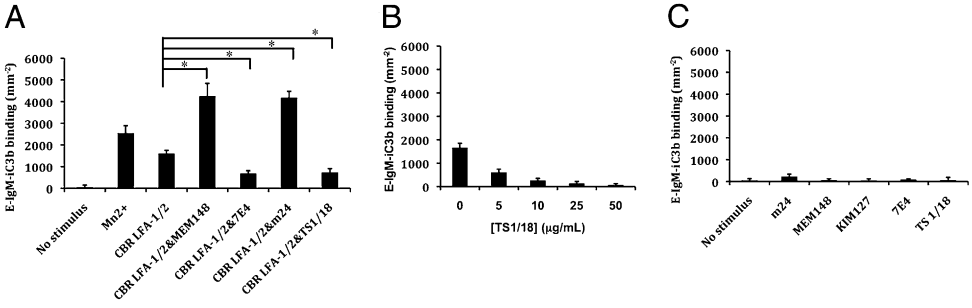


**Fig. 6.** E-IgM-iC3b binding assay. (*A*) Binding of E-IgM-iC3b to $\alpha_x\beta_2$ in the presence of the same combinations of Fabs as used in EM. $Mn^{2+}$ (1 mM) was used as a positive control. *, $P < 0.01$. (*B*) Effect of TS1/18 Fab concentration on binding in the presence of CBR LFA-1/2 Fab. (*C*) Effects of individual Fabs on E-IgM-iC3b binding. Background binding of ~255 cells/mm$^2$ of E-IgM-iC3b to the BSA blocked surface has been subtracted.

and is completely remodeled upon hybrid domain swing-out to the open conformation. 7E4 could bind to bent $\alpha_X\beta_2$, in agreement with the presence of the closed headpiece in the bent conformation of $\alpha_X\beta_2$ (4). TS1/18 also blocks $\beta_2$ integrin activation on intact cells (27, 35). This mAb binds to the residues on the α1- and α7-helices in the βI domain (Fig. 1*E*) (27, 29). Although the residues recognized by TS1/18 are exposed in both the open and closed headpiece, and in the bent integrin conformation (4), the disposition of these residues is significantly altered in shape shifting to the open headpiece (13); accounting for the specificity of TS1/18 for the closed headpiece conformation. TS1/18 could bind to bent $\alpha_X\beta_2$, which is known to have the closed headpiece (4).

Together with the previous functional studies of the four antibodies on intact cells, the EM results suggest that when integrins on cell surfaces have the open headpiece, adhesion is activated, and when integrins on cell surfaces have the closed headpiece, adhesion is inhibited. Furthermore, we correlated the effects of the antibodies on headpiece conformation in EM with their functional effects on E-IgM-iC3b binding to the same $\alpha_X\beta_2$ construct. The extended-open conformation of $\alpha_X\beta_2$ bound iC3b, whereas the bent-closed and the extended-closed conformations of $\alpha_X\beta_2$ did not bind ligand.

The conformational state of an integrin in a functional assay is affected not only by the presence of antibodies specific for a particular headpiece conformation, but also by the presence of ligand. It is well established that ligand binding stabilizes the open headpiece state of integrins $\alpha_V\beta_3$, $\alpha_{IIb}\beta_3$, and $\alpha_5\beta_1$ (6, 11–13). With antibodies specific for the open headpiece present, ligand binding to $\alpha_X\beta_2$ is expected to stabilize and reinforce the activated state with the extended-open conformation. When $\alpha_X\beta_2$ is stabilized in the extended-closed conformation, the presence of ligand is expected to compete with inhibitory Fabs, to favor the open headpiece conformation. We found evidence for a requirement for a higher concentration of inhibitory Fab in the presence of ligand. Thus, a higher concentration of TS1/18 Fab was required to maintain the closed headpiece conformation in the iC3b binding assay, as inferred from the concentration required for full inhibition, than in the EM experiments.

Our studies show that extended $\alpha_X\beta_2$ with a closed headpiece does not represent an intermediate affinity state. The use of an appropriate TS1/18 Fab concentration demonstrated that the extended-closed integrin did not bind ligand and was indistinguishable from the bent conformation in its low affinity for ligand.

Our results define the affinity states of the three major conformational states of an integrin, $\alpha_X\beta_2$. The open and closed headpieces have high and low affinity for ligand, respectively. Although the extended-closed conformation is intermediate in conformation between the bent-closed and extended-open conformations, it is not intermediate in affinity. Like the bent-closed conformation, the extended-closed conformation has low affinity for ligand. However, the observed affinity or adhesiveness of integrins on the cell surface will reflect the proportion of integrins in each specific conformational state. Thus, our data suggest that the extended-closed conformation serves only as a conformational transition state between the bent and the extended-open conformations.

Our data suggest that the intermediate affinity state observed in the literature for the related $\beta_2$ integrin LFA-1 (16–20) does not have to come from an individual conformational state, but could instead result from a mixture of conformational states. Previous studies showed that LFA-1 binding to ICAM-3, compared with ICAM-1, required more activation as defined by the number of activation agents needed (19–21). It was demonstrated that Mg/EGTA is sufficient to activate binding to ICAM-1, but an additional activating mAb is required for ICAM-3. Further experiments showed that an LFA-1 mutant (D790R), which was suggested to be in an extended-closed conformation by reactivity with KIM127 and not MEM148, could bind to ICAM-1, but not ICAM-3 (22). These results were interpreted in support of the hypothesis that the extended-closed conformation of LFA-1 has intermediate affinity. However, the conformation of LFA-1 after binding to ICAM-1 was not defined in these experiments. Our results on $\alpha_X\beta_2$ suggest another interpretation, that the presence of ICAM-1 ligand shifted the equilibrium toward the extended-open conformation and that the affinity of ICAM-3 was not high enough to shift the equilibrium to the open headpiece, thus requiring an additional activation agent for ICAM-3 binding.

Interestingly, 7E4 antibody to the hybrid domain has previously been found to inhibit adhesiveness stimulated by agents that act distally to, but not directly on, the βI domain (26). Here, with activation of $\alpha_X\beta_2$ induced distally by CBR LFA-1/2 Fab, both 7E4 and TS1/18 were found to stabilize the closed headpiece conformation in EM and to abolish adhesiveness to iC3b. The ability of $Mg^{2+}$/EGTA and a $\beta_2$ N351S mutation, both of which act on the βI domain (26, 36), to bypass inhibition by 7E4 (26) suggests that the open conformation of the βI domain, as defined by the conformation of the metal binding sites in the βI domain, can be uncoupled from the open conformation of the headpiece, as defined by hybrid domain swing-out. Such uncoupling has already been observed for $\beta_3$ integrins. Ligand-mimetic antagonists, soaked into crystals can induce substantial remodeling of the βI domain loops around the metal and ligand binding sites, even though hybrid domain swing-out is prevented by crystal lattice contacts (13, 37). Furthermore, in $\beta_2$ integrins, mutations in the $\alpha_L$ I domain can uncouple $\alpha_L$ I domain opening from $\beta_2$ I domain opening (27). In other words, there are conformational equilibria that couple hybrid domain swing-out to the high affinity state of the βI domain and that couple the high affinity state of the βI domain to the high affinity state of the αI domain. Energy input at one end of this system of coupled equilibria and conformational changes should flow predictably to the other end. However, when energy is input in two positions in the system, which favor opposite conformational states, a high energy state may arise, with conformational states present that do not coexist in the low energy state, as described in the examples above. Thus, although our study suggests that the closed state of the headpiece of integrin $\alpha_X\beta_2$ is coupled to the low affinity state of the $\alpha_X$ I domain, it must always be kept in mind that coupling is not absolute, but is through equilibria.

$\alpha_X\beta_2$ binds ligand through its $\alpha_X$ I domain (38). Structures of isolated integrin αI domains have demonstrated three conformational states termed closed, intermediate, and open (1). Although the conformational state of the $\alpha_X$ I domain cannot be resolved in our EM experiments, our combined functional and EM results demonstrate strong coupling between the affinity of the $\alpha_X$ I domain for ligand and the closed and open states of the headpiece. The recently observed flexible interface between the αI and β-propeller domains in $\alpha_X\beta_2$ suggest that both the intermediate and open states of αI domain are compatible with the open headpiece conformation (4). Currently, it is hypothesized that with the headpiece open, the αI domain would be predominantly in an intermediate conformation in absence of ligand binding and in an open conformation in the presence of ligand binding. To date, no mechanism is known for stabilizing the αI domain in three distinct states by inside-out signaling, because only two conformational states of the headpiece are known. Further studies on LFA-1 are important to demonstrate whether the results reported here on $\alpha_X\beta_2$ can be extended to $\alpha_L\beta_2$. Furthermore, X-ray crystallography studies on αI integrins in the activated state are important to further address the coupling between the conformational states of the αI domain and the headpiece.

## Materials and Methods

**Protein Preparation.** The construct and purification procedure of soluble $\alpha_X\beta_2$ ectodomain that contained TEV protease sites, ACID/BASE coiled coils, and Strep-II and His6 tags were described previously (8). The murine mAbs CBR LFA-1/2 (10), KIM127 (39), and TS1/18 (40) have been previously described.

MEM148 (24), 7E4 (41), and m24 (32) are generous gifts from Vaclav Horejsi (Charles University, Prague, Czechoslovakia), Carl G. Gahmberg (University of Helsinki, Finland), and Nancy Hogg (Cancer Research United Kingdom, London Research Institute, United Kingdom), respectively. IgGs were purified with a protein A column. Fab fragments were prepared with bead-immobilized papain using the Pierce Fab preparation kit (Pierce Chemical) (8).

**Negative Stain EM of Integrin–Fab Complexes.** To prepare integrin–Fab complexes, $\alpha_X\beta_2$ (0.2 μg/mL) was incubated with a sixfold molar excess (0.25 μg/mL) of each Fab at 37 °C for 1 h, followed by gel filtration on Superdex 200 HR equilibrated with TBS/Ca/Mg buffer (20 mM Tris-HCl pH 7.5, 150 mM NaCl, 1.0 mM $CaCl_2$, 1.0 mM $MgCl_2$). Peak fractions were adsorbed to glow-discharged carbon-coated copper grids, stained with uranyl formate, and low-dose images acquired with an FEI Tecnai 12 electron microscope at 120 kV and a nominal magnification of 67,000× using a defocus of –1.5 μm.

Image processing was performed with SPIDER and EMAN. 2,000–6,000 particles were interactively collected for each sample using BOXER in EMAN (42) and subjected to multireference alignment and classification with SPIDER (43). The process is similar to that described previously (8), with some changes made to improve the accuracy of classification and alignment and the quality of the class averages. In brief, the coordinates of the picked particles were converted to SPIDER format and used in windowing particles to create a boxed image stack. Each image in the stack was normalized to a mean intensity of 0 and SD of 50. Normalized images were subjected to 10 iterations of centering, multivariate statistical analysis, *K*-means classification, class averaging, and multireference alignment, with the class averages used as input references for multireference alignment in the next iteration. In the *K*-means classification step, the seeds were randomly selected. In the multireference alignment step, a combined translational and rotational search was used to align particles.

**E-IgM-iC3b Adhesion Assay.** Sheep erythrocytes were sensitized with anti-Forssman IgM and C5-deficient human complement (44). Microtiter plate wells were coated overnight at 4 °C with 50 μL of 5 μg/mL rabbit polyclonal anti-velcro (ACID/BASE coiled-coil) antibody (45), and blocked with 1% heat-treated BSA in PBS. A total of 50 μL of 2 μg/mL $\alpha_X\beta_2$ was added for 2 h at 20 °C. After three washes, 50 μL of Fabs (10 μg/mL) or $MnCl_2$ (2.0 mM) was added for 30 min at 37 °C. E-IgM-iC3b (50 μL) was then admixed and plates were incubated for 1 h at 37 °C. Unbound erythrocytes were removed by gentle swirling of the buffer and inverting the plate, followed by washing twice with HBSS/15 mM hepes pH 7.3/1 mM $MgCl_2$/1 mM $CaCl_2$. Bound E-IgM-iC3b were imaged by DIC microscopy and enumerated using ImageJ version 1.41 from the National Institutes of Health.

**ACKNOWLEDGMENTS.** This work was supported by National Institutes of Health Grant AI72765. X.C. is a Pfizer Fellow of Life Sciences Research Foundation. T.W. is an investigator in the Howard Hughes Medical Institute.

1. Luo B-H, Carman CV, Springer TA (2007) Structural basis of integrin regulation and signaling. *Annu Rev Immunol* 25:619–647.
2. Xiong J-P, et al. (2001) Crystal structure of the extracellular segment of integrin αVβ3. *Science* 294:339–345.
3. Zhu J, et al. (2008) Structure of a complete integrin ectodomain in a physiologic resting state and activation and deactivation by applied forces. *Mol Cell* 32:849–861.
4. Xie C, et al. (2010) Structure of an integrin with an αI domain, complement receptor type 4. *EMBO J* 29:666–679.
5. Lu C, Ferzly M, Takagi J, Springer TA (2001) Epitope mapping of antibodies to the C-terminal region of the integrin $\beta_2$ subunit reveals regions that become exposed upon receptor activation. *J Immunol* 166:5629–5637.
6. Takagi J, Petre BM, Walz T, Springer TA (2002) Global conformational rearrangements in integrin extracellular domains in outside-in and inside-out signaling. *Cell* 110: 599–11.
7. Kim M, Carman CV, Springer TA (2003) Bidirectional transmembrane signaling by cytoplasmic domain separation in integrins. *Science* 301:1720–1725.
8. Nishida N, et al. (2006) Activation of leukocyte $\beta_2$ integrins by conversion from bent to extended conformations. *Immunity* 25:583–594.
9. Beglova N, Blacklow SC, Takagi J, Springer TA (2002) Cysteine-rich module structure reveals a fulcrum for integrin rearrangement upon activation. *Nat Struct Biol* 9: 282–287.
10. Petruzzelli L, Maduzia L, Springer TA (1995) Activation of LFA-1 (CD11a/CD18) and Mac-1 (CD11b/CD18) mimicked by an antibody directed against CD18. *J Immunol* 155: 854–866.
11. Takagi J, Strokovich K, Springer TA, Walz T (2003) Structure of integrin $\alpha_5\beta_1$ in complex with fibronectin. *EMBO J* 22:4607–4615.
12. Mould AP, et al. (2003) Structure of an integrin-ligand complex deduced from solution x-ray scattering and site-directed mutagenesis. *J Biol Chem* 278:39993–39999.
13. Xiao T, Takagi J, Coller BS, Wang JH, Springer TA (2004) Structural basis for allostery in integrins and binding to fibrinogen-mimetic therapeutics. *Nature* 432:59–67.
14. Luo B-H, Springer TA, Takagi J (2003) Stabilizing the open conformation of the integrin headpiece with a glycan wedge increases affinity for ligand. *Proc Natl Acad Sci USA* 100:2403–2408.
15. Luo BH, Karanicolas J, Harmacek LD, Baker D, Springer TA (2009) Rationally designed integrin $\beta_3$ mutants stabilized in the high affinity conformation. *J Biol Chem* 284: 3917–3924.
16. Stanley P, et al. (2008) Intermediate-affinity LFA-1 binds alpha-actinin-1 to control migration at the leading edge of the T cell. *EMBO J* 27:62–75.
17. Cairo CW, Mirchev R, Golan DE (2006) Cytoskeletal regulation couples LFA-1 conformational changes to receptor lateral mobility and clustering. *Immunity* 25:297–308.
18. Shamri R, et al. (2005) Lymphocyte arrest requires instantaneous induction of an extended LFA-1 conformation mediated by endothelium-bound chemokines. *Nat Immunol* 6:497–506.
19. Al-Shamkhani A, Law SK (1998) Expression of the H52 epitope on the β2 subunit is dependent on its interaction with the α subunits of the leukocyte integrins LFA-1, Mac-1 and p150,95 and the presence of $Ca^{2+}$. *Eur J Immunol* 28:3291–3300.
20. Hogg N, et al. (1999) A novel leukocyte adhesion deficiency caused by expressed but nonfunctional β2 integrins Mac-1 and LFA-1. *J Clin Invest* 103:97–106.
21. Tang RH, Tng E, Law SK, Tan SM (2005) Epitope mapping of monoclonal antibody to integrin αLβ2 hybrid domain suggests different requirements of affinity states for intercellular adhesion molecules (ICAM)-1 and ICAM-3 binding. *J Biol Chem* 280: 29208–29216.
22. Tang XY, Li YF, Tan SM (2008) Intercellular adhesion molecule-3 binding of integrin αLβ2 requires both extension and opening of the integrin headpiece. *J Immunol* 180: 4793–4804.
23. Ohi M, Li Y, Cheng Y, Walz T (2004) Negative staining and image classification: Powerful tools in modern electron microscopy. *Biol Proced Online* 6:23–34.
24. Drbal K, Angelisová P, Cerný J, Hilgert I, Horejsí V (2001) A novel anti-CD18 mAb recognizes an activation-related epitope and induces a high-affinity conformation in leukocyte integrins. *Immunobiology* 203:687–698.
25. Tan SM, et al. (2001) The N-terminal region and the mid-region complex of the integrin β2 subunit. *J Biol Chem* 276:36370–36376.
26. Tng E, Tan SM, Ranganathan S, Cheng M, Law SK (2004) The integrin αLβ2 hybrid domain serves as a link for the propagation of activation signal from its stalk regions to the I-like domain. *J Biol Chem* 279:54334–54339.
27. Lu C, Shimaoka M, Zang Q, Takagi J, Springer TA (2001) Locking in alternate conformations of the integrin αLβ2 I domain with disulfide bonds reveals functional relationships among integrin domains. *Proc Natl Acad Sci USA* 98:2393–2398.
28. Kamata T, et al. (2002) The role of the CPNKEKEC sequence in the β2 subunit I domain in regulation of integrin αLβ2 (LFA-1). *J Immunol* 168:2296–2301.
29. Huang C, Zang Q, Takagi J, Springer TA (2000) Structural and functional studies with antibodies to the integrin β 2 subunit. A model for the I-like domain. *J Biol Chem* 275: 21514–21524.
30. Luo B-H, Takagi J, Springer TA (2004) Locking the $\beta_3$ integrin I-like domain into high and low affinity conformations with disulfides. *J Biol Chem* 279:10215–10221.
31. Byron A, et al. (2009) Anti-integrin monoclonal antibodies. *J Cell Sci* 122:4009–4011.
32. Dransfield I, Hogg N (1989) Regulated expression of $Mg^{2+}$ binding epitope on leukocyte integrin alpha subunits. *EMBO J* 8:3759–3765.
33. Smith A, et al. (2005) A talin-dependent LFA-1 focal zone is formed by rapidly migrating T lymphocytes. *J Cell Biol* 170:141–151.
34. Koivunen E, et al. (2001) Inhibition of β2 integrin-mediated leukocyte cell adhesion by leucine-leucine-glycine motif-containing peptides. *J Cell Biol* 153:905–916.
35. Beals CR, Edwards AC, Gottschalk RJ, Kuijpers TW, Staunton DE (2001) CD18 activation epitopes induced by leukocyte activation. *J Immunol* 167:6113–6122.
36. Chen JF, Salas A, Springer TA (2003) Bistable regulation of integrin adhesiveness by a bipolar metal ion cluster. *Nat Struct Biol* 10:995–1001.
37. Xiong JP, et al. (2002) Crystal structure of the extracellular segment of integrin αVβ3 in complex with an Arg-Gly-Asp ligand. *Science* 296:151–155.
38. Vorup-Jensen T, Ostermeier C, Shimaoka M, Hommel U, Springer TA (2003) Structure and allosteric regulation of the αXβ2 integrin I domain. *Proc Natl Acad Sci USA* 100: 1873–1878.
39. Robinson MK, et al. (1992) Antibody against the Leu-CAM β-chain (CD18) promotes both LFA-1- and CR3-dependent adhesion events. *J Immunol* 148:1080–1085.
40. Sanchez-Madrid F, et al. (1982) Three distinct antigens associated with human T-lymphocyte-mediated cytolysis: LFA-1, LFA-2, and LFA-3. *Proc Natl Acad Sci USA* 79: 7489–7493.
41. Nortamo P, Patarroyo M, Kantor C, Suopanki J, Gahmberg CG (1988) Immunological mapping of the human leucocyte adhesion glycoprotein gp90 (CD18) by monoclonal antibodies. *Scand J Immunol* 28:537–546.
42. Ludtke SJ, Baldwin PR, Chiu W (1999) EMAN: semiautomated software for high-resolution single-particle reconstructions. *J Struct Biol* 128:82–97.
43. Frank J, et al. (1996) SPIDER and WEB: processing and visualization of images in 3D electron microscopy and related fields. *J Struct Biol* 116:190–199.
44. Bilsland CAG, Diamond MS, Springer TA (1994) The leukocyte integrin p150,95 (CD11c/CD18) as a receptor for iC3b. Activation by a heterologous β subunit and localization of a ligand recognition site to the I domain. *J Immunol* 152:4582–4589.
45. Takagi J, Erickson HP, Springer TA (2001) C-terminal opening mimics 'inside-out' activation of integrin $\alpha_5\beta_1$. *Nat Struct Biol* 8:412–416.

# Supporting Information

## Chen et al. 10.1073/pnas.1008663107

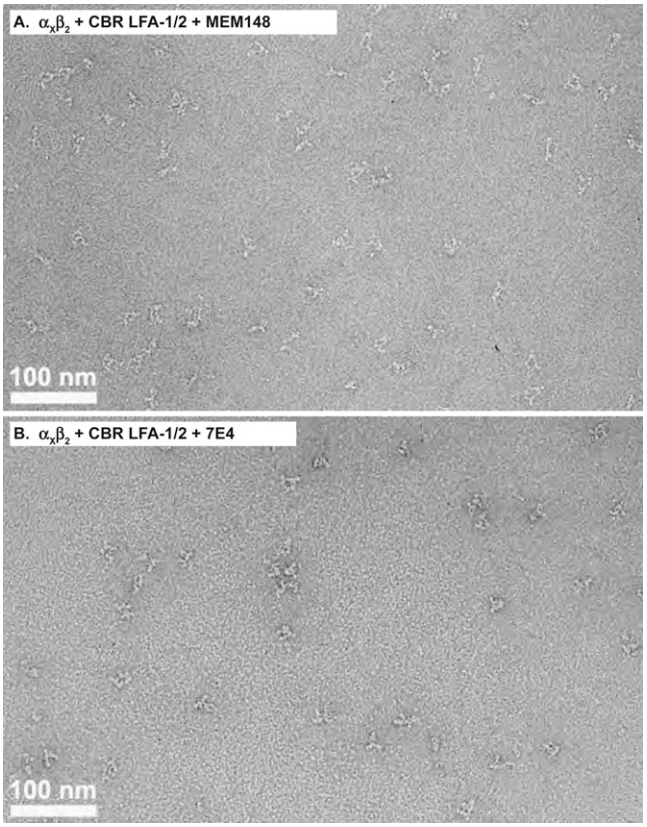


**Fig. S1.** (Continued)

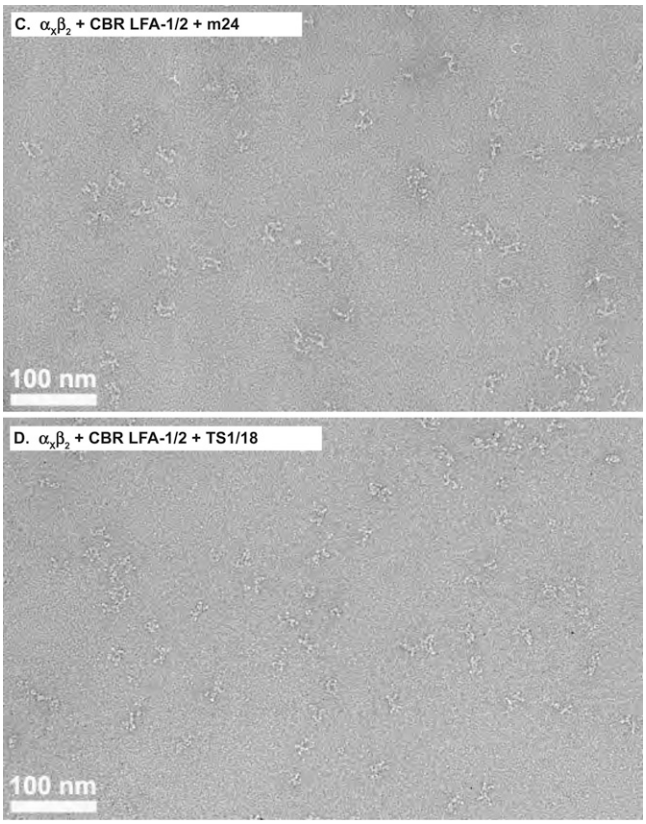


**Fig. S1.** Representative EM raw micrographs of $\alpha_X\beta_2$–Fab complexes. (*A*) $\alpha_X\beta_2$ in complex with CBR LFA-1/2 and MEM148 Fabs. (*B*) $\alpha_X\beta_2$ in complex with CBR LFA-1/2 and 7E4 Fabs. (*C*) $\alpha_X\beta_2$ in complex with CBR LFA-1/2 and m24 Fabs. (*D*) $\alpha_X\beta_2$ in complex with CBR LFA1/2 and TS1/18 Fabs.

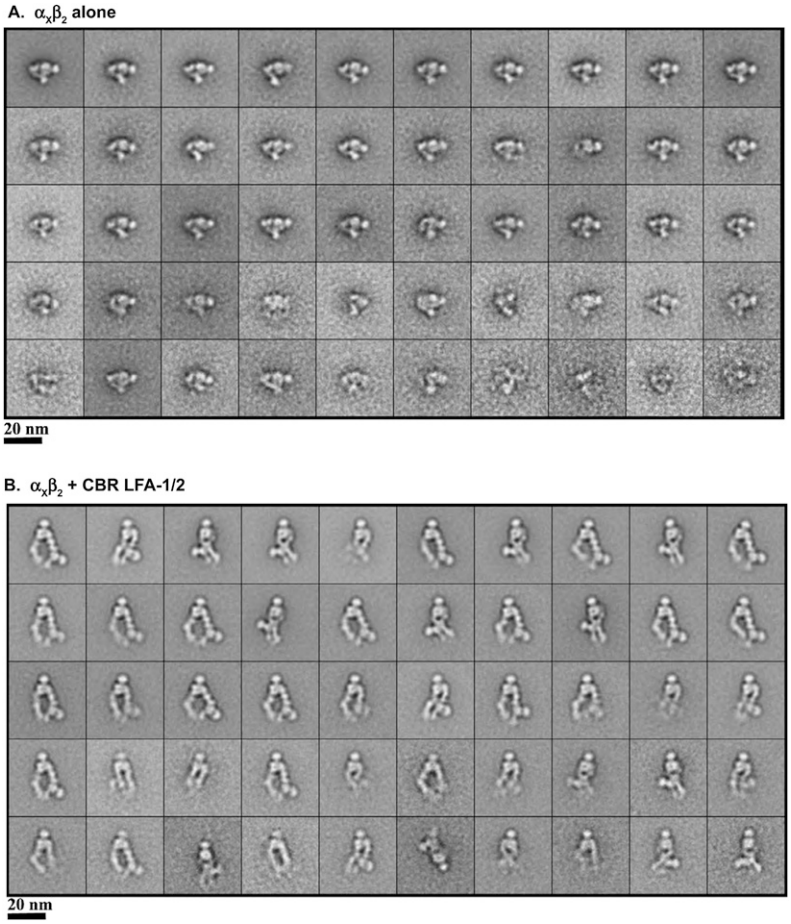


**Fig. S2.** (Continued)

C. $\alpha_x\beta_2$ + CBR LFA-1/2 + MEM148

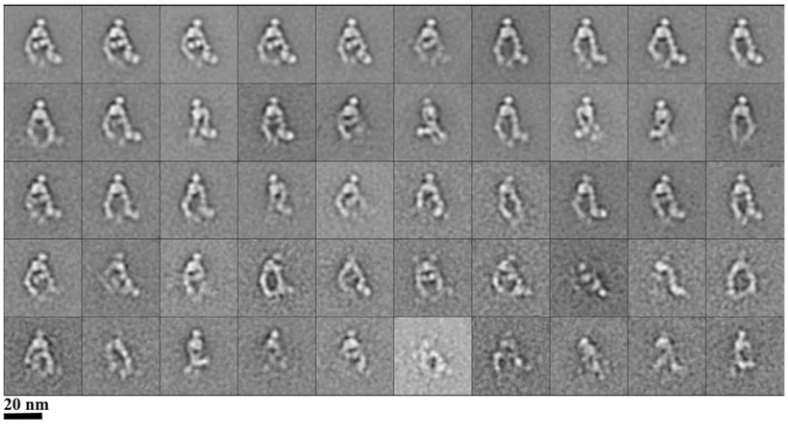

20 nm

D. $\alpha_x\beta_2$ + CBR LFA-1/2 and 7E4

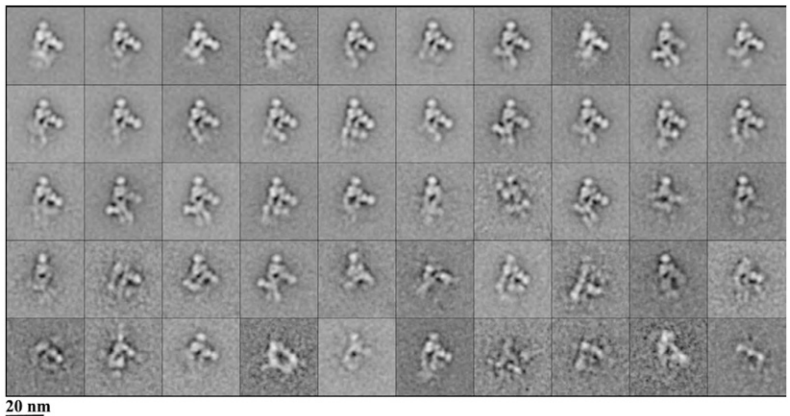

20 nm

**Fig. S2.** (Continued)

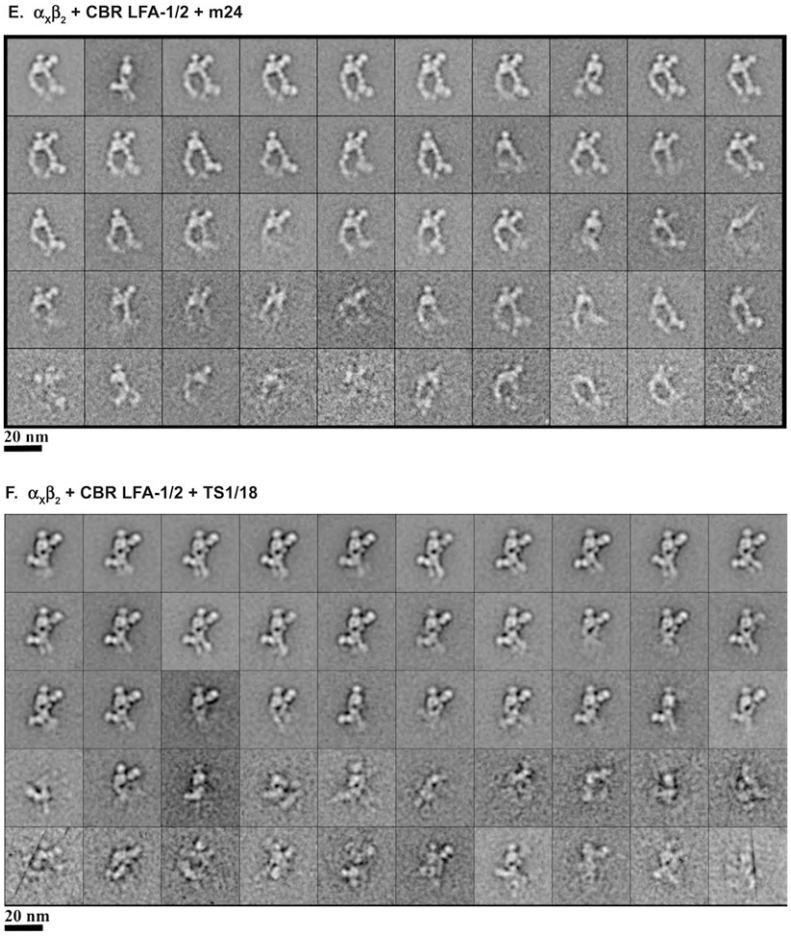


**Fig. S2.** The complete set of class averages. (*A*) Class averages of $\alpha_X\beta_2$ alone. (*B*) Class averages of $\alpha_X\beta_2$ in complex with CBR LFA-1/2 Fab. (*C*) Class averages of $\alpha_X\beta_2$ in complex with CBR LFA-1/2 and MEM148 Fabs. (*D*) Class averages of $\alpha_X\beta_2$ in complex with CBR LFA1/2 and 7E4 Fabs. (*E*) Class averages of $\alpha_X\beta_2$ in complex with CBR LFA-1/2 and m24 Fabs. (*F*) Class averages of $\alpha_X\beta_2$ in complex with CBR LFA-1/2 and TS1/18 Fabs. Averages are ranked (left to right in each row, from top row to bottom row) by numbers of particles in each class.